IJE TRANSACTIONS A: Basics Vol. 28, No. 10, (October 2015) 1533-1542

International Journal of Engineering

Journal Homepage: www.ije.ir

A Non-linear Static Equivalent Model for Multi-layer Annular/Circular Graphene Sheet Based on Non-local Elasticity Theory Considering Third Order Shear Deformation Theory in Thermal Environment

S. Dastjerdi *, M. Jabbarzadeh

Department of Mechanical Engineering, Mashhad Branch, Islamic Azad University, Mashhad, Iran

P A P E R I N F O

Paper history:
Received 15 August 2015
Received in revised form 29 September 2015
Accepted 16 October 2015

Keywords:
Single and Multi-layer Graphene Sheet
Non-local Elasticity Theory of Eringen
Differential Quadrature Method (DQM)
Semi-analytical Polynomial Method (SAPM)
Winkler-pasternak Elastic Foundation
Thermal Environment

A B S T R A C T

In this paper, it is tried to find an approximate single layer equivalent for multi-layer graphene sheets based on third order non-local elasticity theory. The plates are embedded in two parameter Winkler-Pasternak elastic foundation, and also the thermal effects are considered. A uniform transverse load is imposed on the plates. Applying the non-local theory of Eringen based on third order shear deformation theory and considering the van der Waals interaction between the layers, the governing equations are derived for a multi-layer graphene sheet. The governing equations for single layer graphene sheet are obtained by eliminating the van der Waals interaction. In this study, two different methods are applied to solve the governing equations. First, the results are obtained applying the differential quadrature method (DQM), which is a numerical method, and then a new semi-analytical polynomial method (SAPM) is presented. The results from DQM and SAPM are compared and it is concluded that the SAPM results are satisfactorily accurate in comparison with DQM. Since analyzing a multi-layer graphene sheet needs a time-consuming computational process, it is investigated to find an appropriate thickness for a single layer sheet to equalize the maximum deflections of multi-layer and single layer sheets. It is concluded that by considering a constant value of the van der Waal interaction between the layers, the maximum deflections of multi and single layer sheets are equal in a specific thickness of the single layer sheet.

***doi**: 10.5829/idosi.ije.2015.28.10a.18*

1. INTRODUCTION

Nowadays, nano structures are applied widely in areas such as nanotubes, nanobeams and nanoplates. The graphene sheets are kind of nanomaterials which are formed in hexagonal shape by covalent bonds between carbon atoms. Special properties of graphene sheets such as high strength, low weight to area ratio, unique and extraordinary electrical properties attracted many researchers to consider this topic as their major activities [1-3]. The bending strength of graphene sheet is low, so using multi-layers of graphene sheets improves this weakness. In order to make multi-layers of graphene sheet, several single layers of graphene are set on each other by weak van der Waals bond between the surface atoms [4].

There are different methods to analyze the nanostructures [5]. In addition to experimental methods, there are atomic modelling [6], combination of atomic modelling and continuum mechanics [7] and continuum mechanics [8]. Since controlling experimental and atomic modelling is difficult and computations are expensive, consequently, the continuum mechanics method is used by many researchers because of convenience in formulations and acceptable results in comparison with two other methods [9]. The continuum mechanics method is categorized in three different methods: 1- couple stress theory [10], 2-modified strain gradient theory [11], and 3-The Eringen non-local elasticity theory [12]. The Eringen non-local elasticity theory is widely used to analyze the mechanical

*Corresponding Author's Email *dastjerdi_shahriar@yahoo.com* (Sh. Dastjerdi)

Please cite this article as: S. Dastjerdi, M. Jabbarzadeh, Symmetrical A Non-linear Static Equivalent Model for Multi-layer Annular/Circular Graphene Sheet Based on Non-local Elasticity Theory Considering Third Order Shear Deformation Theory (TSDT) in Thermal Environment, International Journal of Engineering (IJE), TRANSACTIONS A: Basics Vol. 28, No. 10, (October 2015) 1533-1542

behavior of nanostructures. Eringen theory by considering the small scale effects, explains that the stress in a reference point is affected by the strains in whole body domain or the interactive bonds between the carbon atoms are not neglected and have significant effects on mechanical behavior in nano scales. So, using classical elasticity theory generates unacceptable results [13].

Pradhan [14] investigated the buckling of rectangular graphene sheets, considering the isotropic material properties and the third order shear deformation theory (TSDT). They showed that using TSDT plate theory for moderately thick plates renders more accurate results. Shen Shen [15] studied bending, vibrations and post buckling of rectangular graphene plates resting on elastic foundation, using classical plate theory by considering the nonlinear strains field in thermal environment. Ansari et al. [16] proposed an analytical solution to calculate the critical buckling load for a mono layered graphene sheet under uniform loading by use of Galerkin method. Hosseini-hashemi et al. [17] investigated the buckling of rectangular graphene plates using the Mindlin and Eringen non-local elasticity theories. The results are compared with Euler-Bernoulli, CLPT and higher order shear deformation theories. Zhou et al. [18] studied the bending of bi-layer graphene sheets under transverse loading in thermal environment. The nonlinear strains field and CLP theory are used by these authors and they showed that the small scale effects play an important role in nonlinear bending analysis of graphene sheets. Zenkour et al. [19] investigated the thermal buckling of nanoplates embedded in an elastic Winkler-Pasternak matrix, using the sinusoidal shear deformation plate theory and compared the results with comparison with classical plate theory (CLPT) or first order shear deformation theory (FSDT) theories. Jomehzadeh and Saidi [20] studied the large amplitude vibrations of bi-layer graphene sheets embedded in a nonlinear polymer matrix. The nonlinear bending analysis of mono layered sector graphene sheets embedded in an elastic matrix is investigated by Dastjerdi et al. [21]. They proved that the maximum deflection decreases as well as the increase of non-local parameter. Also, in that paper, the results for local and non-local elasticity theories are compared.

In this study, it is investigated to a multi-layer graphene sheet with an equivalent single layer in thermal environment has been modelled. To study the small scale effects on the results, the third order non-local theory of Eringen is applied. The material properties are assumed to be orthotropic. The DQM and a new semi-analytical polynomial method (SAPM) are applied to solve the governing equations. It is concluded that it is possible to calculate the specific thickness for a single layer graphene sheet, that the deflections of the single and the multi-layer sheets would be equal. Consequently, to avoid the vast computational process for analyzing the multi-layers, an appropriate equivalent single layer graphene sheet can be applied.

2. FORMULATION

A multi-layer annular/circular graphene sheet with thickness *h*, inner radius r_i , outer radius r_o , under uniform transverse loading *q* is shown in Figure 1. In this paper, the third order shear deformation theory (TSDT) is applied to obtain the governing equations because the thickness must be varied for single layer sheet and TSDT gives more accurate results in CLPT or FSDT. TSDT does not have the weaknesses of the other theories by considering the shear stress effects through the thickness of the plate (weakness of the CLPT) and satisfying the boundary condition for shear stress at the surfaces of the plate (weakness of FSDT). According to the third-order shear deformation theory, the displacement field can be expressed as follow. The index *i* represents the layer number, for example *i=1* refers to the upper layer under transverse load and *i=n* the bottom layer rested on the elastic foundation (*i=1, 2, 3… n*).

$$Ui(r,z) = ui(r) + z\psi i_1(r) + z^3\psi i_2(r) \quad (1)$$

$$Vi(r,z) = 0 \quad (2)$$

$$Wi(r,z) = wi(r) \quad (3)$$

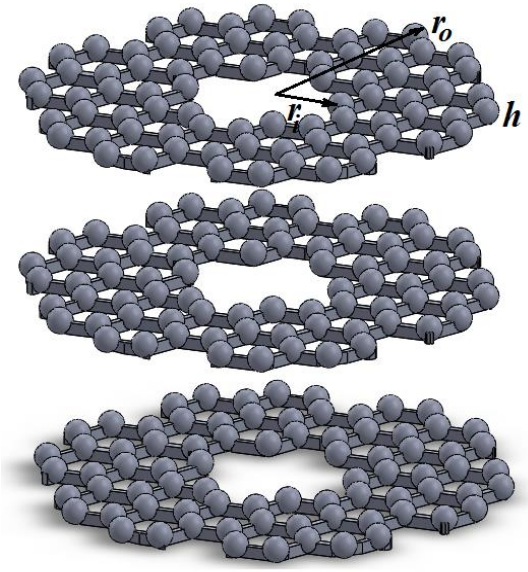

Figure 1. Geometry of multi-layer annular/circular graphene sheet

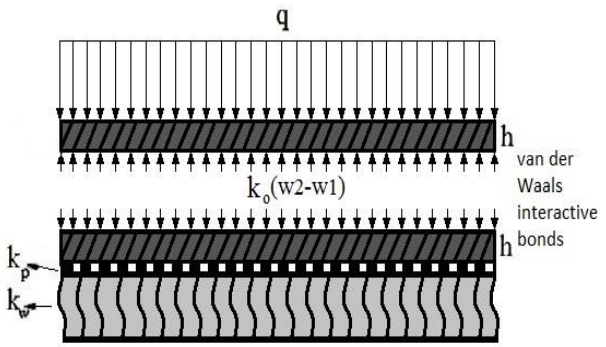

Figure 2. Bi-layer graphene sheet rested on Winkler-Pasternak elastic foundation regarding the van der Waals interaction between the layers

The van der Waals interaction and elastic matrix are pictured in Figure 2. k_w and k_p are the Winkler and Pasternak stiffness coefficients of elastic foundation, respectively. The term $k_o(w_2 - w_1)$ refers to the van der Waals interaction bonds between the layers in Figure 2. k_o is the van der Waals stiffness.

In Equations (1)-(3), *ui* and *wi* are the displacement components of the mid-plane along the *r* and *z* directions, respectively. ψi_1 explains the rotation functions of the transverse normal about circumferential and radial directions. Here, ψi_2 is the only mathematical parameter. Considering the von-Karman assumptions, the strain fields are expressed as follows:

$$\varepsilon i_r = \frac{\partial ui}{\partial r} + z\frac{\partial \psi i_1}{\partial r} + z^3\frac{\partial \psi i_2}{\partial r} + \frac{1}{2}\left(\frac{dwi}{dr}\right)^2 - \alpha\cdot\Delta T \quad (4)$$

$$\varepsilon i_\theta = \frac{ui}{r} + z\frac{\psi i_1}{r} + z^3\frac{\psi i_2}{r} - \alpha\cdot\Delta T \quad (5)$$

$$\gamma i_{rz} = \frac{dwi}{dr} + \psi i_1 + 3z^2\psi i_2 \quad (6)$$

where $\alpha\cdot\Delta T$ is thermal strain, in which α is thermal diffusivity and ΔT the temperature difference. The effects of atomic forces is significant in nano scales and it must be entered into the fundamental relations as material parameters [12, 21]. In non-local theory, the stress at reference point *X* is a function of strain field in every point on the sheet. Eringen presented a differential form of the non-local relations as follows [12]:

$$\left(1-\mu\nabla^2\right)\sigma i^{NL} = \sigma i^{L} = C:\varepsilon, \mu = (e_0 a)^2 \quad (7)$$

$$C = \begin{bmatrix} \frac{E_r}{1-\nu_{r\theta}\nu_{\theta r}} & \frac{\nu_{r\theta}E_\theta}{1-\nu_{r\theta}\nu_{\theta r}} & 0 \\ 0\frac{\nu_{r\theta}E_\theta}{1-\nu_{r\theta}\nu_{\theta r}} & \frac{E_\theta}{1-\nu_{r\theta}\nu_{\theta r}} & 0 \\ 0 & 0 & G_{rz} \end{bmatrix}$$

In Equation (7), a is internal characteristic length, and e_0 is material constant which is determined by experiment. The parameter $e_0 a$ is the nan-local parameter exposing the small-scale effect on the nano-size structures. The value of the non-local parameter depends on boundary conditions, chirality, number of walls, and the nature of motions and often is taken between 0 to 2 nm [22]. By applying Equation (7), the non-local stress components can be expressed in cylindrical coordinates system below [12]:

$$\sigma i_r^{NL} - \mu\left(\nabla^2\sigma i_r^{NL} - \frac{4}{r^2}\frac{\partial \sigma i_{r\theta}^{NL}}{\partial\theta} - \frac{2}{r^2}\left(\sigma i_r^{NL} - \sigma i_\theta^{NL}\right)\right) = \sigma i_r^{L} \quad (8)$$

$$\sigma i_\theta^{NL} - \mu\left(\nabla^2\sigma i_\theta^{NL} + \frac{4}{r^2}\frac{\partial \sigma i_{r\theta}^{NL}}{\partial\theta} + \frac{2}{r^2}\left(\sigma i_r^{NL} - \sigma i_\theta^{NL}\right)\right) = \sigma i_\theta^{L} \quad (9)$$

$$\sigma i_{rz}^{NL} - \mu\left(\nabla^2\sigma i_{rz}^{NL} - \frac{1}{r^2}\sigma i_{rz}^{NL} - \frac{2}{r^2}\frac{\partial \sigma i_{\theta z}^{NL}}{\partial\theta}\right) = \sigma i_{rz}^{L} \quad (10)$$

∇^2 is the Laplacian operator in cylindrical coordinates system which is defined below:

$$\nabla^2 = \frac{d^2}{dr^2} + \frac{1}{r}\frac{d}{dr} \quad (11)$$

The non-local stress resultant components $Ni_j^{NL}, Mi_j^{NL}, Hi_j^{NL}(j = r,\theta)$ and Q_r^{NL}, Y_r^{NL} can be formulated as follows:

$$(Mi_r, Mi_\theta)^{NL} = \int_{-\frac{h}{2}}^{\frac{h}{2}}\left(\sigma i_r, \sigma i_\theta\right)^{NL} z\,dz \quad (12)$$

$$(Ni_r, Ni_\theta, Qi_r)^{NL} = \int_{-\frac{h}{2}}^{\frac{h}{2}}\left(\sigma i_r, \sigma i_\theta, \sigma i_{rz}\right)^{NL} dz \quad (13)$$

$$Yi_r^{NL} = \int_{-\frac{h}{2}}^{\frac{h}{2}}\sigma i_{rz}^{NL} z^2 dz \quad (14)$$

$$(Hi_r, Hi_\theta)^{NL} = \int_{-\frac{h}{2}}^{\frac{h}{2}}\left(\sigma i_r, \sigma i_\theta\right)^{NL} z^3 dz \quad (15)$$

Substituting Equations (8)-(10) into Equations (12)-(15), the local and non-local force, moment and shear

force components can be developed as follows:

$$\begin{aligned}&\left(Ni,Mi,Hi\right)_r^{NL}-\mu\Bigg(\nabla^2\left(Ni,Mi,Hi\right)_r^{NL}-\frac{4}{r^2}\\&\frac{\partial\left(Ni,Mi,Hi\right)_{r\theta}^{NL}}{\partial\theta}-\frac{2}{r^2}\Big(\left(Ni,Mi,Hi\right)_r^{NL}\\&-\left(Ni,Mi,Hi\right)_\theta^{NL}\Big)\Bigg)=\left(Ni,Mi,Hi\right)_r^{L}\end{aligned}\tag{16}$$

$$\begin{aligned}&\left(Ni,Mi,Hi\right)_\theta^{NL}-\mu\Bigg(\nabla^2\left(Ni,Mi,Hi\right)_\theta^{NL}+\frac{4}{r^2}\\&\frac{\partial\left(Ni,Mi,Hi\right)_{r\theta}^{NL}}{\partial\theta}+\frac{2}{r^2}\Big(\left(Ni,Mi,Hi\right)_\theta^{NL}\\&-\left(Ni,Mi,Hi\right)_\theta^{NL}\Big)\Bigg)=\left(Ni,Mi,Hi\right)_\theta^{L}\end{aligned}\tag{17}$$

$$\left(Qi,Yi\right)_{rz}^{NL}-\mu\left(\nabla^2\left(Qi,Yi\right)_{rz}^{NL}-\frac{1}{r^2}\left(Qi,Yi\right)_{rz}^{NL}\right)=\left(Qi,Yi\right)_{rz}^{L}\tag{18}$$

$Ni_j^{\,L},Mi_j^{\,L},Hi_j^{\,L}\,(j=r,\theta)$ and $Qi_r^{\,L},Yi_r^{\,L}$ are the local form of stress resultants which are defined for orthotropic material below:

$$\begin{aligned}&Ni_r^{\,L}=\frac{E_r h}{1-\nu_{r\theta}\nu_{\theta r}}\left(\frac{dui}{dr}+\frac{1}{2}\left(\frac{dwi}{dr}\right)^2-\alpha\cdot\Delta T\right)+\\&\frac{\nu_{r\theta}E_\theta h}{1-\nu_{r\theta}\nu_{\theta r}}\left(\frac{ui}{r}-\alpha\cdot\Delta T\right)\end{aligned}\tag{19}$$

$$\begin{aligned}&Ni_r^{\,L}=\frac{\nu_{r\theta}E_\theta h}{1-\nu_{r\theta}\nu_{\theta r}}\left(\frac{dui}{dr}+\frac{1}{2}\left(\frac{dwi}{dr}\right)^2-\alpha\cdot\Delta T\right)+\\&\frac{E_\theta h}{1-\nu_{r\theta}\nu_{\theta r}}\left(\frac{ui}{r}-\alpha\cdot\Delta T\right)\end{aligned}\tag{20}$$

$$Qi_r^{\,L}=\frac{1}{4}G_{rz}\psi i_2 h^3+G_{rz}h\left(\frac{dwi}{dr}+\psi i_1\right)\tag{21}$$

$$Yi_r^{\,L}=\frac{3}{80}G_{rz}\psi i_2 h^5+\frac{1}{12}G_{rz}h^3\left(\frac{dwi}{dr}+\psi i_1\right)\tag{22}$$

$$\begin{aligned}&Mi_r^{\,L}=\frac{h^5}{80\left(1-\nu_{r\theta}\nu_{\theta r}\right)}\left(E_r\frac{d\psi i_2}{dr}+\frac{\nu_{r\theta}E_\theta}{r}\psi i_2\right)+\\&\frac{h^3}{12\left(1-\nu_{r\theta}\nu_{\theta r}\right)}\left(E_r\frac{d\psi i_1}{dr}+\frac{\nu_{r\theta}E_\theta}{r}\psi i_1\right)\end{aligned}\tag{23}$$

$$\begin{aligned}&Mi_\theta^{\,L}=\frac{h^5}{80\left(1-\nu_{r\theta}\nu_{\theta r}\right)}\left(\nu_{r\theta}E_\theta\frac{d\psi i_2}{dr}+\frac{E_\theta}{r}\psi i_2\right)+\\&\frac{h^3}{12\left(1-\nu_{r\theta}\nu_{\theta r}\right)}\left(\nu_{r\theta}E_\theta\frac{d\psi i_1}{dr}+\frac{E_\theta}{r}\psi i_1\right)\end{aligned}\tag{24}$$

$$\begin{aligned}&Hi_r^{\,L}=\frac{h^7}{448\left(1-\nu_{r\theta}\nu_{\theta r}\right)}\left(E_r\frac{d\psi i_2}{dr}+\frac{\nu_{r\theta}E_\theta}{r}\psi i_2\right)\\&+\frac{h^5}{80\left(1-\nu_{r\theta}\nu_{\theta r}\right)}\left(E_r\frac{d\psi i_1}{dr}+\frac{\nu_{r\theta}E_\theta}{r}\psi i_1\right)\end{aligned}\tag{25}$$

$$\begin{aligned}&Hi_\theta^{\,L}=\frac{h^7}{448\left(1-\nu_{r\theta}\nu_{\theta r}\right)}\left(\nu_{r\theta}E_\theta\frac{d\psi i_2}{dr}+\frac{E_\theta}{r}\psi i_2\right)\\&+\frac{h^5}{80\left(1-\nu_{r\theta}\nu_{\theta r}\right)}\left(\nu_{r\theta}E_\theta\frac{d\psi i_1}{dr}+\frac{E_\theta}{r}\psi i_1\right)\end{aligned}\tag{26}$$

In this study, the governing equations and also the boundary conditions are derived based on the principle of minimum total potential energy, respectively. The basic relations are presented as follows:

$$\delta\Pi i=\delta Ui+\delta\Omega i=0\tag{27}$$

$$\delta Ui=\iiint_v\left(\sigma i_r^{\,NL}\delta\varepsilon i_r+\sigma i_\theta^{\,NL}\delta\varepsilon i_\theta+\sigma i_{rz}^{\,NL}\delta\gamma i_{rz}\right)dV\tag{28}$$

$$\delta\Omega 1=\int_{r_i}^{r_o}\int_0^{2\pi}\left(q+k_o\left(w_2-w_1\right)\right)\delta w r dr d\theta\quad\text{Upper layer}\tag{29}$$

$$\begin{aligned}&\delta\Omega i=\int_{r_i}^{r_o}\int_0^{2\pi}\left(-k_o\left(w_i-w_{i-1}\right)+k_o\left(w_{i+1}-w_i\right)\right)\delta w r dr d\theta\\&\left(i=2...n-1\right),\text{Second layer down to the layer before the bottom layer}\end{aligned}\tag{30}$$

$$\begin{aligned}&\delta\Omega n=\int_{r_i}^{r_o}\int_0^{2\pi}\left(-k_o\left(w_n-w_{n-1}\right)-k_w w_n+k_p\nabla^2 w_n\right)\\&\delta w r dr d\theta\quad\text{Bottom layer}\end{aligned}\tag{31}$$

U and Ω are the internal strain energy and potential of external applied forces, respectively.

Using the variation principals, the governing equations of multi-layer annular/circular graphene sheets are obtained in cylindrical coordinates system in terms of local force, moment and the shear force resultants by substituting Equations (16)-(18) into the non-local form of the governing equations as follow:

$$\delta ui:Ni_{r,r}^{\,L}+\frac{1}{r}\left(Ni_r^{\,L}-Ni_\theta^{\,L}\right)=0\tag{32}$$

$$\begin{aligned}&\delta w_1:Q1_{r,r}^{L}+\frac{1}{r}Q1_r^{L}+\left(1-\mu\nabla^2\right)\left(q+k_o\left(w_2-w_1\right)\right.\\&\left.+N1_r^{L}\frac{1}{r}\frac{dw_1}{dr}+N1_{r,r}^{L}\frac{dw_1}{dr}+N1_r^{L}\frac{d^2w_1}{dr^2}\right)=0\quad\text{Upper layer}\end{aligned}\tag{33}$$

$$\begin{aligned}&\delta w_i:Qi_{r,r}^{\,L}+\frac{1}{r}Qi_r^{\,L}+\left(1-\mu\nabla^2\right)\left(-k_o\left(w_i-w_{i-1}\right)\right.\\&+k_o\left(w_{i+1}-w_i\right)+Ni_r^{\,L}\frac{1}{r}\frac{dw_1}{dr}+Ni_{r,r}^{\,L}\frac{dw_i}{dr}\\&\left.+Ni_r^{\,L}\frac{d^2w_i}{dr^2}\right)=0,\qquad i=2...n-1\end{aligned}\tag{34}$$

$$\delta w_n : Qn_{r,r}^L + \frac{1}{r}Qn_r^L + \left(1-\mu\nabla^2\right)\left(k_p\nabla^2 w_n - k_w w_n - k_o\left(w_n - w_{n-1}\right) + Nn_r^L\frac{1}{r}\frac{dw_n}{dr} + Nn_{r,r}^L\frac{dw_n}{dr} + Nn_r^L\frac{d^2w_n}{dr^2}\right) = 0 \quad \text{Bottom layer} \tag{35}$$

$$\delta\psi i_1 : Mi_{r,r}^L + \frac{1}{r}\left(Mi_r^L - Mi_\theta^L\right) - Qi_r^L = 0 \tag{36}$$

$$\delta\psi i_2 : Hi_{r,r}^L + \frac{1}{r}\left(Hi_r^L - Hi_\theta^L\right) - 3Yi_r^L = 0 \tag{37}$$

Since the numbers are extremely small in nano scales, due to convenience and to avoid the digits error in processing, the non-dimensional terms are introduced as follows. After substituting these terms into the resultant components and then into the governing equations (Equations (32)-(37)), the dimensionless form of equations would be obtained in terms of displacements and rotations.

$$r^* = \frac{r}{r_o}; ui^* = \frac{ui}{h}; wi^* = \frac{wi}{r_o}; z^* = \frac{z}{h}; \psi i_1^* = \psi i_1; \psi_2^* = \frac{\psi_2}{h^2}$$

$$\eta = \frac{h}{r_o};\ \mu^* = \frac{\mu}{r_o^2};\ q^* = \frac{q}{E_r};\ k_w^* = \frac{k_w r_o}{E_r}; k_p^* = \frac{k_p}{E_r h}$$

$$\rho 1 = \frac{E_\theta}{E_r}; \rho 2 = \frac{G_{rz}}{E_r}; \upsilon = 1 - \nu_{r\theta}\nu_{\theta r}$$

3. NUMERICAL SOLUTION

In this study, two different methods are applied to solve the governing equations. First the DQM [23, 24] which is an accurate numerical method is used to obtain the results. In addition, a new semi-analytical polynomial method (SAPM) is presented [21]. The SAPM is based on the definition of polynomials. Consider a general ordinary differential equation as follow:

$$g_1(r)\frac{df(r)}{dr} + g_2(r)\frac{d^2f(r)}{dr^2} + \ldots + g_n(r)\frac{d^nf(r)}{dr^n} + h(r) = 0, \quad r_i \le r \le r_o \tag{38}$$

The domain $r_i \le r \le r_o$ is divided to *N* grid point. The function *f(r)* is defined for SAPM as follow:

$$f(r) = \sum_{i=1}^{N} a_i r^{(i-1)} \quad r_i \le r \le r_o \tag{39}$$

By substituting Equation (39) into Equation (38), the differential equation will be transformed to the algebraic equation as follow:

$$g_1(r)\frac{d}{dr}\left(\sum_{i=1}^{N} a_i r^{(i-1)}\right) + g_2(r)\frac{d^2}{dr^2}\left(\sum_{i=1}^{N} a_i r^{(i-1)}\right) + \ldots + g_n(r)\frac{d^n}{dr^n}\left(\sum_{i=1}^{N} a_i r^{(i-1)}\right) + h(r) = 0, \quad r_i \le r \le r_o \tag{40}$$

For an *n* order differential equation, *n* number of boundary conditions in boundary points r_i and r_o are needed. For example, for a second order differential equation the value of function or derivative of *f(r)* in boundaries are known (dark points in Figure 3.). Consequently, two algebraic equations in boundaries would be determined and the remaining equations can be derived from Equation (40) for inner grid points (bright points in Figure 3.). Now, there are a set of *N* algebraic equations and *N* unknown constant $a_i, i = 1,2,..,N$. This method is one of the simplest methods for solving the differential equations. If a set of differential equations system is considered, the procedure is similar to the mentioned explanations.

$$ui^* = \sum_{i=1}^{N} a_i r^{(i-1)} \tag{41}$$

$$wi^* = \sum_{i=1}^{N} a_{(i+N)} r^{(i-1)} \tag{42}$$

$$\psi i_1^* = \sum_{i=1}^{N} a_{(i+2N)} r^{(i-1)} \tag{43}$$

$$\psi i_2^* = \sum_{i=1}^{N} a_{(i+3N)} r^{(i-1)} \tag{44}$$

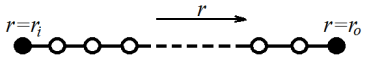

Figure 3. The division of one directional domain for ODE problems

Now, by substituting u^*, w^*, ψ_1^* and ψ_2^* as polynomial functions into Equations (32)-(37), the differential van der Waals interaction between the layers is an obstacle for increase of the upper layer's defection. Consequently, with increasing k_o, decreases the maximum deflection of the upper layer. On the contrary, the deflection of the middle and bottom layer is increased. Totally, the deflection of the upper, middle and bottom layers converges along the rise of the van der Waals interaction. The final converged deflection for triple layer is about 25 percent less than the bi-layer sheet. On the other hand, the strength of the mentioned bi-layer sheet is increased about 25 percent by adding another sheet.

The van der Waals interaction between the layers is an obstacle for increase of the upper layer's defection. Consequently, with rise of k_o, the maximum deflection of the upper layer decreases. On the contrary, the deflection of the middle and bottom layer is increased. Totally, the deflection of the upper, middle and bottom layers converges along the rise of the van der Waals

interaction. The final converged deflection for triple layer is about 25 percent less than the bi-layer sheet. On the other hand, the strength of the mentioned bi-layer sheet is increased about 25 percent by adding another sheet. Equations will be transformed to nonlinear algebraic equations system. In this paper, the Newton-Raphson method is applied to solve the nonlinear set of algebraic equations.

4. BOUNDARY CONDITIONS

The boundary conditions are derived from Equations (27)-(31) in the category of the simply supported (S), clamped (C) and free edges (F). The definition for the boundary conditions is shown in Figure 4.

S: $u = w = M_r = H_r = 0 \qquad r = r_i, r_o$

C: $u = w = \psi_1 = \psi_2 = 0 \qquad r = r_i, r_o$

F: $N_r = Q_r = M_r = H_r = 0 \qquad r = r_i, r_o$

5. NUMERICAL RESULTS AND DISSCUSION

A single layer graphene sheet is considered. Figure 5 demonstrates the comparison between the maximum deflection of the plate due to applying SAPM and DQM, and also shows their rate of convergences. The material properties of the plate are as follows:

$E_r = 1.06\times10^{12}$ Pa; $E_\theta = 0.85\times10^{12}$ Pa; $\nu_{r\theta} = \nu_{\theta r} = 0.3$

$q^* = 1\times10^7 / E$; $k_w = 1.13$GPa/nm; $k_p = 1.13$Pa.m

$\alpha = 2.02\times10^{-6}$; $\Delta T = 1000$ C^o; $r_i / r_o = 0.2$

It is observed that the satisfactory convergence of the results is acquired only for number of nine grid points.

Also, there is not any distinctive differences about the rate of convergence for different types of boundary conditions. The results of two methods are remarkably close to each other. Consequently, applying the SAPM is suggested because of considerably convenience in formulation, accurate results combined with high rate of convergence in comparison with DQM. The comparison between FSDT and TSDT analyses is shown in Table 1 for various conditions. The results of TSDT are smaller than FSDT. There is shear stress distribution on the surfaces of the plate in FSDT analysis and this issue is one of the weaknesses of this theory. So, the results of TSDT analysis are more accurate in comparison with FSDT. According to Table 1, it is concluded that the TSDT and FSDT results are closer for SS types of boundary conditions in compare to CC. This means that the two theories approached for more flexible boundary conditions. Also, the FSDT and TSDT analysis distance with increase of the non-local parameter, temperature differences and thickness of the plate.

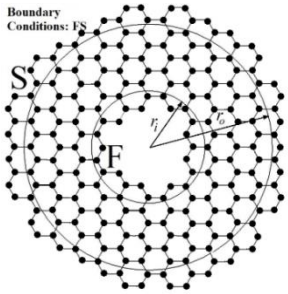

Figure 4. Definition of the boundary conditions

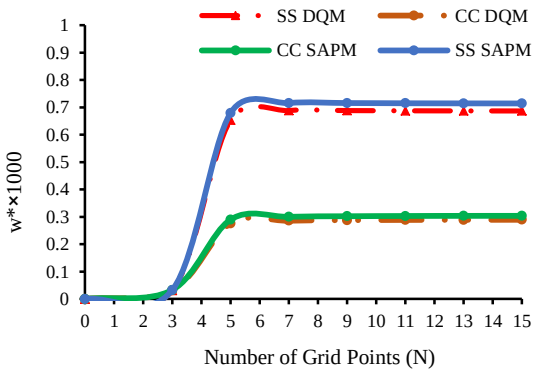

Figure 5. Variation of dimensionless deflection versus the number of grid points for DQM and SAPM domain

The effect of increasing the non-local parameter on decreasing the R_{TF} is more than that of the temperature differences. Also, the increase of the thickness has the most effects on R_{TF}. In this study, because of analyzing a multi-layer graphene sheet needs the vast computational process, it is aimed to find an equivalent thickness for single layer graphene sheet, so the thickness is varied to model a multi-layer sheet. Consequently, according to the conclusions presented in Table 1, the TSDT analysis is applied for obtaining more accurate results. A bi-layer and triple layer annular graphene sheet is considered with SS boundary conditions. The variation of dimensionless deflection versus the van der Waals interaction between the layers is indicated in Figure 6 (a) bi-layer and (b) triple layer sheet (e0a=0.5nm) percent by adding another sheet.

The Vander Waals interaction between the layers is an obstacle for increase of the upper layer's defection. Consequently, with rise of k_o, the maximum deflection of the upper layer decreases. On the contrary, the deflection of the middle and bottom layer is increased. Totally, the deflection of the upper, middle and bottom layers converges along the rise of the van der Waals interaction. The final converged deflection for triple layer is about 25 percent less than the bi-layer sheet. On the other hand, the strength of the mentioned bi-layer sheet is increased about 25 percent.

TABLE 1. Comparison of the dimensionless deflection between the FSDT and TSDT analysis for various conditions

		W*×1000		
	e0a	TSDT	FSDT	R_{TF}=TSDT/FSDT
		h = 0.34 nm, α = 2.02e-6, ΔT = 1000 C^o		
CC	0	0.3332001	0.3397170	0.981
	1	0.2876501	0.2983927	0.964
	1.5	0.2477621	0.2592102	0.956
	2	0.2084938	0.2191122	0.951
SS	0	0.8937144	0.8961018	0.997
	1	0.6880056	0.7039360	0.977
	1.5	0.5376839	0.5548085	0.969
	2	0.4100916	0.4275798	0.959
	ΔT C^o	h = 0.34 nm, α = 2.02e-6, e0a = 1 nm		
CC	0	0.228284	0.235063	0.971
	100	0.233106	0.240153	0.970
	500	0.254582	0.262944	0.968
	1000	0.287650	0.298392	0.964
SS	0	0.550740	0.552993	0.996
	100	0.561810	0.565112	0.994
	500	0.611230	0.619406	0.987
	1000	0.688001	0.703936	0.977
	h*= h/(0.34nm)	ΔT = 1000 C^o , α = 2.02e-6, e0a = 1 nm		
CC	1	0.287650	0.298392	0.964
	5	0.010866	0.012916	0.841
	10	0.004138	0.005302	0.781
	100	0.000340	0.000490	0.693
SS	1	0.688005	0.703936	0.977
	5	0.021715	0.023766	0.914
	10	0.005991	0.007030	0.852
	100	0.000348	0.000493	0.704

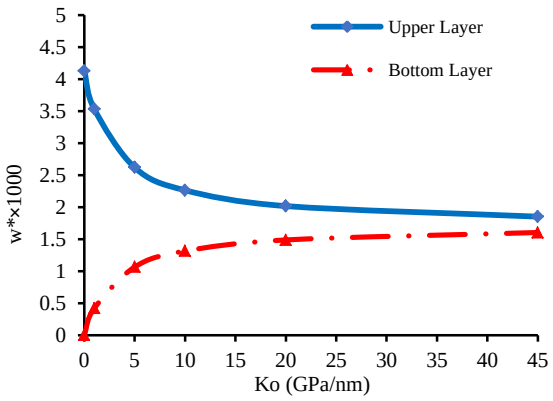

(a)

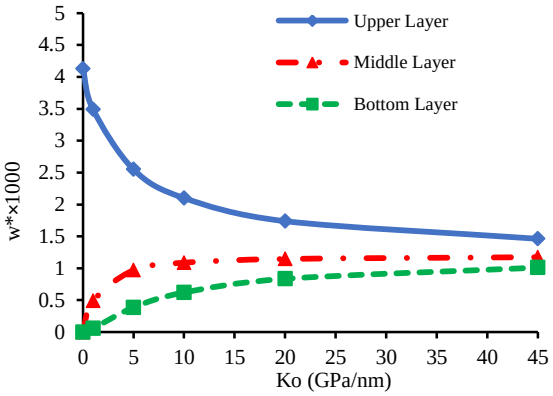

(b)

Figure 6. Variation of dimensionless deflection versus the van der Waals interaction between the layers (a) bi-layer (b) triple layer sheet

Now, it is investigated to find an equivalent thickness for a single layer graphene sheet in order to have equal maximum deflection with the bi-layer sheet. The van der Waals interaction between the layers is a constant value $k_o = 45$ GPa/nm [22]. Figures 7 (a-e) approximate the value for the equivalent thickness in various conditions such as non-local parameter, boundary conditions, loading, temperature differences (ΔT) and the value of the Winkler and Pasternak elastic foundation.

According to Figure 7 (a), it is observed that the equivalent thickness for SS boundary conditions is about $h^* = 1.1$. However, $h^* = 1.16$ is for CC. It is concluded that the more flexible boundary condition is smaller than the equivalent thickness ($e_0 a = 0.5$nm). The effect of small scales is studied in Figure 7 (b). It is seen that with increase of the non-local parameter, the equivalent thickness is decreased. It means that the equal deflections for single and bi-layer sheets will achieve smaller value of equivalent thickness.

The increase of the value of elastic foundation and the temperature differences (ΔT), have the reduction effects on the equivalent thickness (Figure 7 (c, d)). However, according to Figure 7(e), it is observed that the loading does not have any effects on the equivalent thickness. On the other hand, the equivalent thickness remains unchanged with the increase of loading.

The investigation for modelling of a triple layer graphene sheet with a single layer is shown in Figure 8. By comparing Figure 7 (b) and Figure 8, it is concluded that addition of a layer to the bi-layer sheet, the equivalent thickness increases about 11 percent for the value of non-local parameter $e_0 a = 0$. It was observed that the equivalent thickness is about 22 percent more than that of the single layer in Figure 7 (b) for bi-layer sheet. Consequently, it can be possible to predict the

behavior of a multi-layer graphene sheet according to this procedure for every condition. On the other hand, a single layer sheet can be studied instead of the multi-layer sheet by predicting the equivalent thickness.

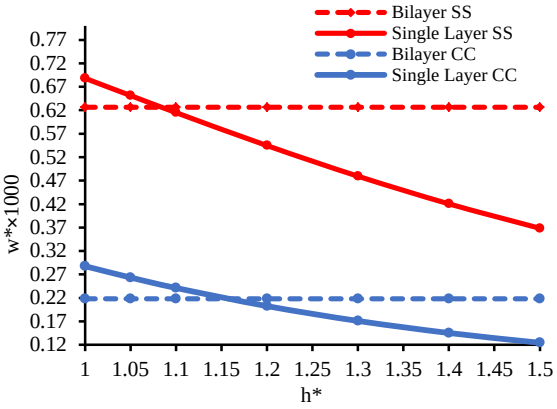

(a)

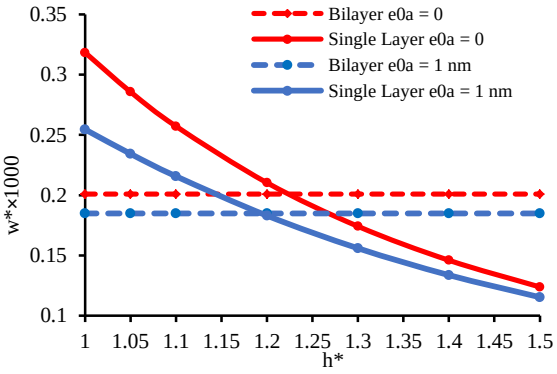

(b)

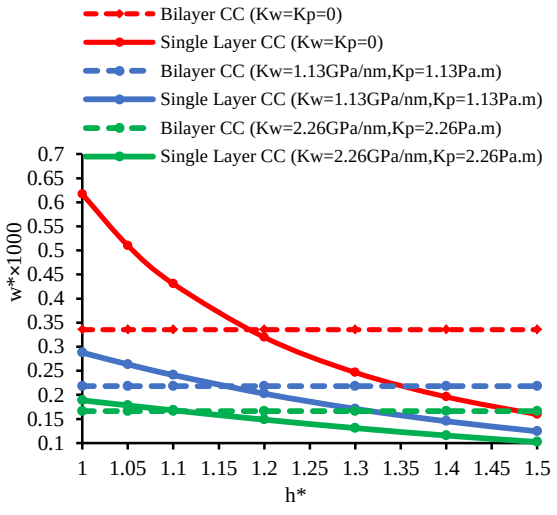

(c)

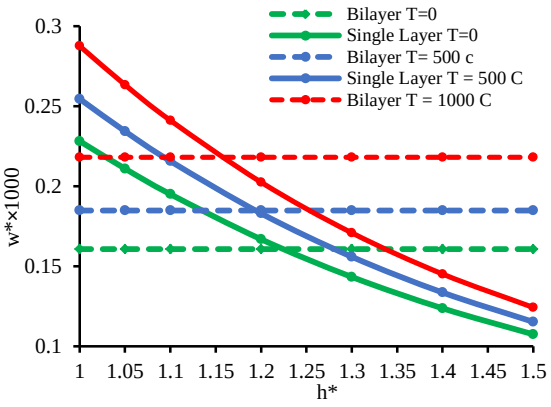

(d)

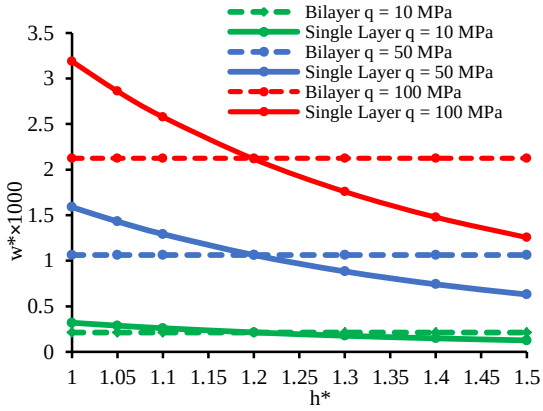

(e)

Figure 7. Variation of dimensionless deflection versus the equivalent thickness for bi-layer graphene sheet (a) different types of boundary conditions (b) different non-local parameter (c) different value of elastic foundation (d) different temperature difference (e) different value of transverse loading

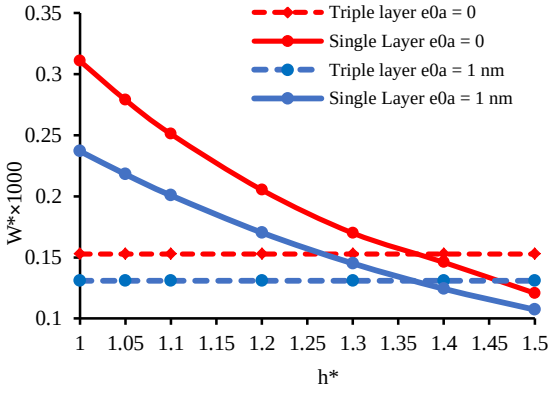

Figure 8. Variation of dimensionless deflection versus the equivalent thickness for triple graphene sheet (CC boundary conditions)

6. CONCLUSION

In this paper, it was tried to find an equivalent single layer graphene sheet to model the multi-layer sheet considering the constant value of the van der Waals interaction between the layers. The plates were embedded in two parameter Winkler and Pasternak elastic matrix in thermal environment. The non-local theory of Eringen were applied based on the third order shear deformation theory of the plates (TSDT) and applying the nonlinear Von-Karman strain field. The equilibrium equations were derived for multi-layer graphene sheet and solved by two methods DQM and SAPM. The most significant conclusions can be categorized as follows:

- The introduced method (SAPM) is extremely accurate, significantly simpler in formulations and coding by computer programs, and its rate of processing time is more than DQM.
- The TSDT results are considerably smaller than that of the FSDT for high value of thicknesses of single layer sheet.
- The deflection of the layers converges for multi-layer graphene sheet with increase of the van der Waals interaction between the layers.
- The equivalent thickness decreases with rise of small scale effects, the value of elastic foundation and temperature differences (ΔT).
- The equivalent thickness remains constant with growing of the transverse load.
- The deflection of a multi-layer sheet is not equal to a single layer with the same thicknesses.
- It is possible to predict an equivalent thickness for a single layer sheet and studying the multi-layer sheet with the equivalent thickness instead of investigation of the multi-layer sheet which needs the time-consuming computational process.

Some of the possible directions for future study can be mentioned below:

1. Providing the general diagrams of equivalent thickness for various conditions.
2. Studying a rectangular or sector graphene sheet instead of the annular/circular sheet.
3. Modeling a multi-layer graphene sheet with a single layer, in vibration and buckling analysis.

7. REFERENCES

1. Lee, C., Wei, X., Kysar, J.W. and Hone, J., "Measurement of the elastic properties and intrinsic strength of monolayer graphene", ***science***, Vol. 321, No. 5887, (2008), 385-388.
2. Robinson, J.T., Zalalutdinov, M., Baldwin, J.W., Snow, E.S., Wei, Z., Sheehan, P. and Houston, B.H., "Wafer-scale reduced graphene oxide films for nanomechanical devices", ***Nano Letters***, Vol. 8, No. 10, (2008), 3441-3445.
3. Bunch, J.S., Van Der Zande, A.M., Verbridge, S.S., Frank, I.W., Tanenbaum, D.M., Parpia, J.M., Craighead, H.G. and McEuen, P.L., "Electromechanical resonators from graphene sheets", ***Science***, Vol. 315, No. 5811, (2007), 490-493.
4. Behfar, K. and Naghdabadi, R., "Nanoscale vibrational analysis of a multi-layered graphene sheet embedded in an elastic medium", ***Composites Science and Technology***, Vol. 65, No. 7, (2005), 1159-1164.
5. Arash, B. and Wang, Q., "A review on the application of nonlocal elastic models in modeling of carbon nanotubes and graphenes", ***Computational Materials Science***, Vol. 51, No. 1, (2012) 303-313.
6. Liew, K., Wong, C., He, X., Tan, M. and Meguid, S., "Nanomechanics of single and multiwalled carbon nanotubes", ***Physical Review B***, Vol. 69, No. 11, (2004), 115429.
7. Wan, H. and Delale, F., "A structural mechanics approach for predicting the mechanical properties of carbon nanotubes", ***Meccanica***, Vol. 45, No. 1, (2010), 43-51.
8. Sun, C. and Liu, K., "Vibration of multi-walled carbon nanotubes with initial axial loading", ***Solid state Communications***, Vol. 143, No. 4, (2007), 202-207.
9. JafarSadeghi-Pournaki, I., Zamanzadeh, M., Madinei, H. and Rezazadeh, G., "Static pull-in analysis of capacitive fgm nanocantilevers subjected to thermal moment using eringen's nonlocal elasticity", ***International Journal of Engineering-Transactions A :Basics***, Vol. 27, No. 4, (2013), 633-640.
10. Ke, L.-L., Wang, Y.-S., Yang, J. and Kitipornchai, S., "Free vibration of size-dependent mindlin microplates based on the modified couple stress theory", ***Journal of Sound and Vibration***, Vol. 331, No. 1, (2012), 94-106.
11. Akgoz, B. and Civalek, O., "A size-dependent shear deformation beam model based on the strain gradient elasticity theory", ***International Journal of Engineering Science***, Vol. 70, (2013), 1-14.
12. Eringen, A.C., "Nonlocal continuum field theories, Springer Science & Business Media, (2002).
13. Eringen, A.C., "Nonlocal continuum mechanics based on distributions", ***International Journal of Engineering Science***, Vol. 44, No. 3, (2006), 141-147.
14. Pradhan, S. and Murmu, T., "Small scale effect on the buckling of single-layered graphene sheets under biaxial compression via nonlocal continuum mechanics", ***Computational Materials Science***, Vol. 47, No. 1, (2009), 268-274.
15. Shen, H.-S., "Nonlocal plate model for nonlinear analysis of thin films on elastic foundations in thermal environments", ***Composite Structures***, Vol. 93, No. 3, (2011), 1143-1152.
16. Ansari, R. and Rouhi, H., "Explicit analytical expressions for the critical buckling stresses in a monolayer graphene sheet based on nonlocal elasticity", ***Solid State Communications***, Vol. 152, No. 2, (2012), 56-59.
17. Hashemi, S.H. and Samaei, A.T., "Buckling analysis of micro/nanoscale plates via nonlocal elasticity theory", ***Physica E: Low-dimensional Systems and Nanostructures***, Vol. 43, No. 7, (2011), 1400-1404.
18. Xu, Y.-M., Shen, H.-S. and Zhang, C.-L., "Nonlocal plate model for nonlinear bending of bilayer graphene sheets subjected to transverse loads in thermal environments", ***Composite Structures***, Vol. 98, (2013), 294-302.
19. Zenkour, A. and Sobhy, M., "Nonlocal elasticity theory for thermal buckling of nanoplates lying on winkler–pasternak elastic substrate medium", ***Physica E: Low-dimensional Systems and Nanostructures***, Vol. 53, (2013), 251-259.
20. Jomehzadeh, E ,.Saidi, A. and Pugno, N., "Large amplitude vibration of a bilayer graphene embedded in a nonlinear

polymer matrix", ***Physica E: Low-dimensional Systems and Nanostructures***, Vol. 44, No. 10, (2012), 1973-1982.

21. Dastjerdia, S., Jabbarzadeh, M. and Tahanib ,M., "Nonlinear bending analysis of sector graphene sheet embedded in elastic matrix based on nonlocal continuum mechanics".
22. Pradhan, S. and Phadikar, J., "Small scale effect on vibration of embedded multilayered graphene sheets based on nonlocal continuum models", ***Physics Letters A***, Vol. 373, No. 11, (2009), 1062-1069.
23. Bellman, R. and Casti, J., "Differential quadrature and long-term integration", ***Journal of Mathematical Analysis and Applications***, Vol. 34, No. 2, (1971), 235-238.
24. Bellman, R., Kashef, B. and Casti, J., "Differential quadrature: A technique for the rapid solution of nonlinear partial differential equations", ***Journal of Computational Physics***, Vol. 10, No. 1, (1972), 40-52.

A Non-linear Static Equivalent Model for Multi-layer Annular/Circular Graphene Sheet Based on Non-local Elasticity Theory Considering Third Order Shear Deformation Theory in Thermal Environment

S. Dastjerdi, M. Jabbarzadeh

Department of Mechanical Engineering, Mashhad Branch, Islamic Azad University, Mashhad, Iran

P A P E R I N F O

Paper history:
Received 15 August 2015
Received in revised form 29 September 2015
Accepted 16 October 2015

Keywords:
Single and Multi-layer Graphene Sheet
Non-local Elasticity Theory of Eringen
Differential Quadrature Method (DQM)
Semi-analytical Polynomial Method (SAPM)
Winkler-pasternak Elastic Foundation
Thermal Environment

چکیده

در این پژوهش تلاش شده است ورق چند لایه گرافن با یک ورق تک لایه بر اساس تئوری الاستیسیته غیرموضعی با به کار گیری تئوری مرتبه سوم تغییر شکل برشی معادل¬سازی شود. ورق مورد بررسی بر روی پایه الاستیک وینکلر- پسترناک و در محیط حرارتی تحت بار عرضی یکنواخت قرار گرفته است. روابط تعادل برای ورق چند لایه گرافن بر اساس تئوری الاستیسیته غیرموضعی مرتبه سوم برشی و با در نظر گرفتن نیروی واندروالس بین لایه¬ها به دست آمده است. با نادیده گرفتن نیروی واندروالس، روابط حاکم برای ورق تک لایه حاصل می¬شوند. در این تحقیق از دو روش مختلف برای حل معادلات حاکم استفاده شده است. ابتدا نتایج با استفاده از روش عددی مربعات دیفرانسیلی(DQM) به دست آمده و سپس یک روش نیمه تحلیلی (SAPM) ارائه شده است. نتایج به دست آمده از دو روش با یکدیگر مقایسه و ملاحظه گردید نتایج روش SAPM با روابط ساده¬تر نسبت به DQM از دقت و همگرایی مناسبی برخوردار می‌باشد. از آنجا که تحلیل ورق¬های چندلایه، از حجم محاسبات گسترده برخوردار بوده و در نتیجه زمان بسیار طولانی را صرف می¬کند، در این تحقیق با تغییر ضخامت ورق تک لایه، یک ضخامت معادل محاسبه گردیده است، بطوری که خیز بیشینه دو ورق چند و تک لایه برابر هم شوند. نتایج حاصل نشان می¬دهد که با ثابت انگاشتن نیروی واندروالس بین لایه¬ها، خیز بیشینه ورق¬های چند و تک لایه در یک ضخامت مشخص برای ورق تک لایه با یکدیگر برابر می¬باشند.

***doi**: 10.5829/idosi.ije.2015.28.10a.18*